

* Correspondence to anna.fontcuberta-morral@epfl.ch

SUPPLEMENTARY INFORMATION

Polarization response of nanowires *à la carte*

Alberto Casadei,¹ Esther Alarcon Llado,¹ Francesca Amaduzzi,¹ Eleonora Russo-Averchi,¹
Daniel Ruffer,¹ Martin Heiss,¹ Luca Dal Negro,^{2,3} and Anna Fontcuberta i Morral*¹

¹*Laboratoire des Matériaux Semiconducteurs, Institut des Matériaux,
École Polytechnique Fédérale de Lausanne, CH-1015 Lausanne, Switzerland*

²*Department of Electrical and Computer Engineering and Photonics Center,
Boston University, 8 Saint Marys Street, Boston, MA, 02215, USA*

³*Division of Materials Science and Engineering, Boston University,
15 Saint Marys Street, Brookline, MA 02446, USA*

SI 1: Bow-tie antennas geometry

The interaction of incident light in the device is calculated with COMSOL Multiphysics by using the electromagnetic waves module and the frequency domain study based on Maxwell's equations. In particular we solve the following equation for the three spatial dimensions:

$$\nabla \times \mu_r^{-1} (\nabla \times E) - k_0^2 \left(e_r - \frac{j \cdot \sigma}{w \cdot e_0} \right) E = 0 \quad (1)$$

where $\mu_r = 1$ (for all materials) is the magnetic permittivity, E is the electric field, k_0 is the wave-vector, e_r and e_0 are the relative and absolute permittivity and $\sigma = \sigma_s + w \cdot e_0 \cdot e_{imm}$ is the electrical conductivity. σ_s is the static conductivity, it is negligible for GaAs, glass and air and it is $\sigma_s = 4 \cdot 10^7 S/m$ in the case of gold. $e_r = (n - i \cdot k)^2$, where n and k are the dielectric real and imaginary part of the material and for gold and GaAs these values are delivered from Palik[E. D. Palik, *Handbook of Optical Constants of Solids*. (Academic Press; 1 edition, 1997)]. Although the nanowire have a 40 nm doped shell with a concentration of $2.2 \times 10^{18} atoms/cm^3$, the doping is only affecting the NW optical properties for wavelength very close to the band-gap[H. C. Casey, D. D. Sell, and K. W. Wecht, *Journal of applied physics* 46, 250 (1975)]. Since in our work we are not interested in this particular task we consider the doping effect negligible on the nanowire optical properties. Plane wave excitation is perpendicularly incident on the NW-nanoantennas system, made of on an hexagonal cross section NW and bow-tie nanoantennas. The nanoantennas are appositely designed with a rounded shaped edges with 15 nm radius in order to better simulate the real device. Periodic continuity conditions are introduced on the surfaces that limit the NW length in order to obtain an infinitely long NW/nanoantennas array and the boundary conditions $E_x = E_y = E_z = 0$ are set along the other external simulation surfaces. A free tetrahedral mesh is used for all the domains with size below 20 nm in the nanowire and respectively bigger sizes for nanoantennas, substrate and surrounding air.

Figure 1a shows the range of geometrical parameters investigated in the calculations. Figure 1b) reports the energy density in a single NW and a device NW/nanotennas in function of the NW diameter. For very small diameters ($< 40 nm$) the nanoantennas enhance the energy density by more than 26 times. Despite the large energy density enhancement, GaAs NWs with small diameter are not optimal candidates for the investigation of opto-electrical properties. Infact, the presence of surface states generates a depletion region that completely inhibits the electrical transport. On the other hand for big diameters ($> 250 nm$)

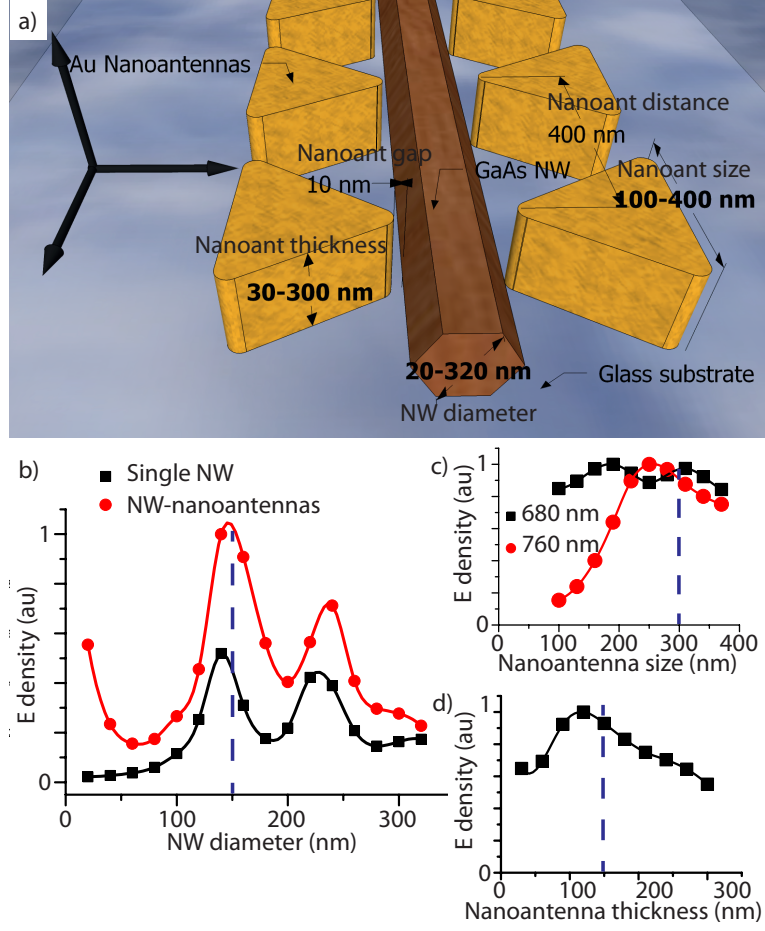


FIG. 1. a) NW-nanoantennas geometry scheme. In bold are represented the range of parameters we investigate in the simulations b),c) and d). Simulations show the electric field energy density inside the NW for transverse polarized incident light with $\lambda = 680$ nm in function of NW diameter (b), nanoantennas size (c) and nanoantennas thickness (d). The effect of the nanoantennas size (c) is also shown for $\lambda = 760$ nm. The blue dot lines indicate the parameter chosen for the realization of the devices.

the distance between the two nanoantenna sides becomes very large, breaking the nanoantennas resonances and leading to an inefficient coupling. For 150 nm in diameter we have the higher electric field energy density and we then use this value for the device fabrication. Fig. 1c and 1d show how the energy density changes in function of the nanoantennas size and thickness and the dimensions selected for the devices fabrication are represented by the blue dashed lines. Also in these cases the parameters chosen for the device realization are selected to maximize the absorption.

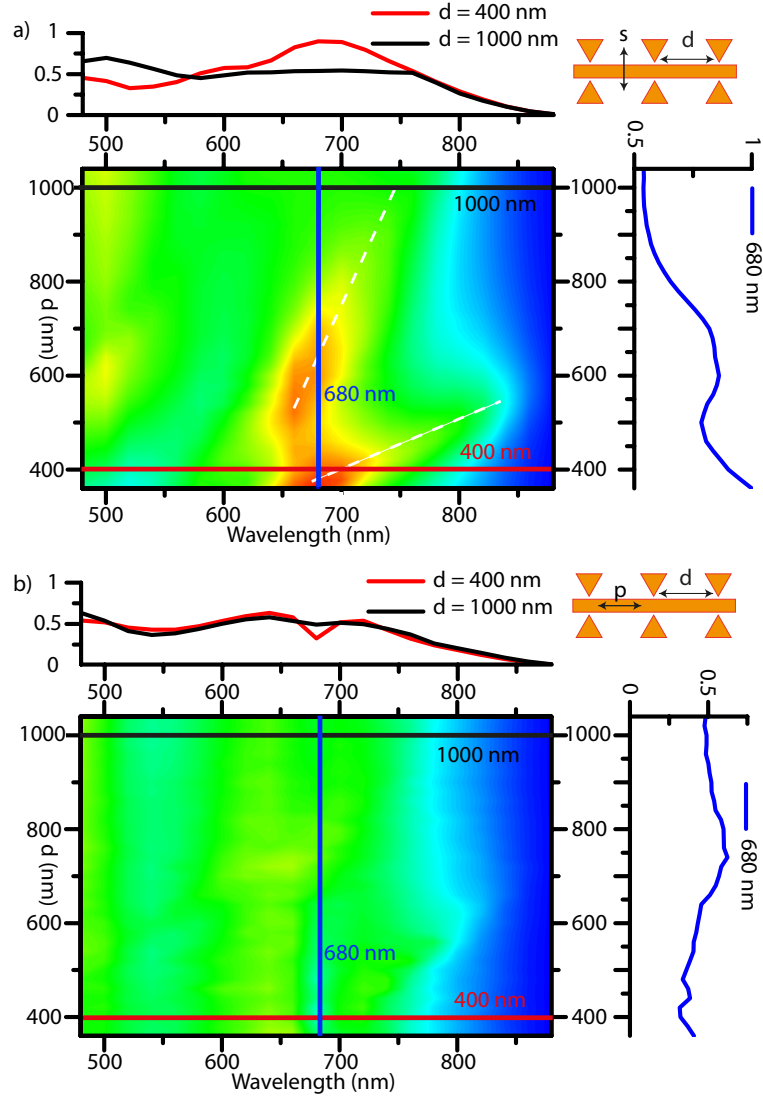


FIG. 2. Calculated absorption efficiency map for a NW/nanoantennas system on a glass substrate as a function of the nanoantenna distance d (represented in the insets) for s-polarization (a) and p-polarization (b). The intensity profiles are taken at 680 nm wavelength and for $d = 400$ and 1000 nm. The dashed lines are used as a guide to the eye in the identification of the guided modes.

The nanoantenna distance d is directly linked to their density along the NW. For small distances ($d = 400$ nm) the density is high, and therefore we expect the largest effects on the NW absorption. We calculated the field energy density in the NW for the distance of 400 nm and we find the largest absorption for transverse polarized light at $\lambda = 680$ nm (fig. 1b). Here we notice that the total nanoantenna dimension along its axis is around 680 nm

and only transverse polarized wavelengths above this dimension can activate the antenna dimer and efficiently enhance the NW absorption. For λ below 680 nm the nanoantennas produce a small reduction in the calculated absorption of the system, while for $\lambda > 680 \text{ nm}$ the absorption enhancement is extended to the infrared with some dependance on the nanoantennas density. As a general rule, in order to enhance the absorption for smaller wavelengths, nanoantennas with smaller dimensions need to be designed.

The absorption efficiency maps (fig. 2a - 2b) show the perfect dipole nanoantennas behavior. Bow-tie nanoantennas actively couple the incident light into the NW only when the light polarization is along the nanoantennas dimer axis and they do not interfere in the NW absorption of the light polarized in the perpendicular direction. In fact they are totally inactive for longitudinal polarized light leaving unaltered the NW absorption but they are efficiently coupling into the NW the transverse polarized light. The profile curves on top show the absorption spectra for the system $d = 400 \text{ nm}$ and $d = 1000 \text{ nm}$, corresponding to the dimensions used for the device fabrication. Finally we notice that the absorption efficiency profiles for $d = 1000 \text{ nm}$ and transverse polarized light is perfectly homogeneous between 550 and 750 nm wavelength.

SI 2: Nanowire absorption modes

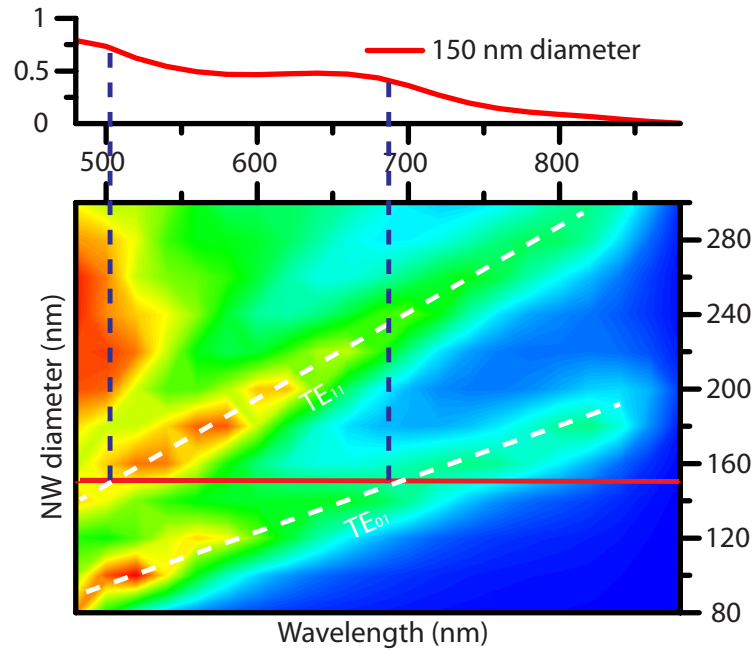


FIG. 3. Calculated absorption efficiency map of a NW laying on a glass substrate under transverse polarized incident light. The white dots lines are guide to the eyes to indicate the NW modes TE_{01} and TE_{11} . The absorption profile is taken for a NW with diameter of 150 nm and the blue dots line show the guided modes position.

SI 3: Electric field energy into the nanowire

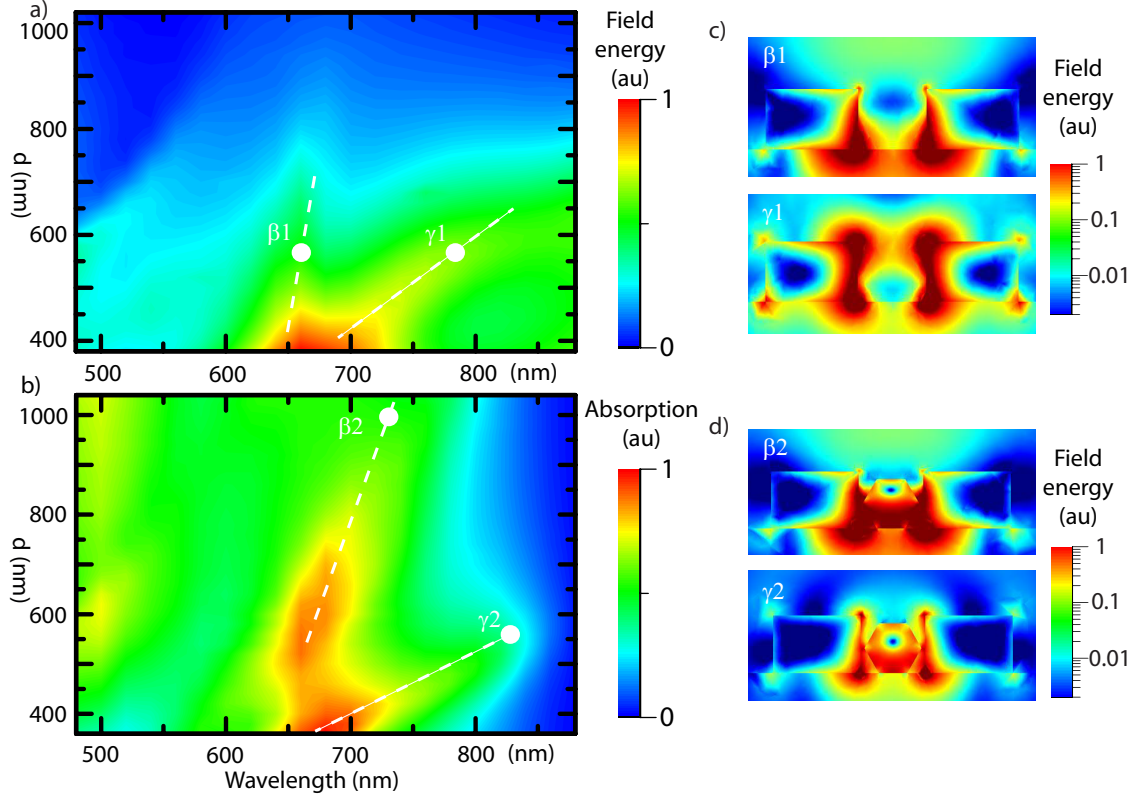


FIG. 4. a) Field energy map for transverse polarization in the system with only nanoantennas in function of the wavelength and the nanoantennas distance. The electric field intensity is integrated on the volume that would correspond to the nanowire volume in the system NW-nanoantennas. b) Map of the nanowire absorption for transverse polarized light. c) and d) show the field energy distribution along the system cross section for the corresponding white points of figure a) and b).

Bow-tie antennas have the ability to concentrate the incoming light in a sub-wavelength volume corresponding to the gap region. We can observe this capability from the field energy distribution in fig. 4c, where β_1 and γ_1 are the corresponding point of fig. 4a. Although the energy is concentrated in the gap region it is also extremely localized along the gold antennas edges. GaAs nanowires have a dielectric constant almost 13 times higher than the one of vacuum and by embedding a nanowire in the antenna array it acts as a cavity, which collects the electric field energy. This behaviour is shown in fig. 4. We observe in fig. 4c that the absorption modes are wider and more pronounced in presence of the nanowire and the

energy field distribution is now localized inside the nanowire beside to the antennas edges (fig. 4d).

SI 4: Scanning photocurrent

Here we demonstrate that bow-tie nanoantennas are able to extremely localize the incoming light into the NW. As a proof of increased photo-current in sub-wavelength NW regions we performed photo-scanning electrical measurements. We use a piezo-stage to automatically scan the laser spot around the device, while collecting the current at each position. The scan was taken with steps of 200 nm . We use a 100X objective (NA 0.75) to focus the laser on the sample. The laser spot is diffraction limited and is approximatively $1\ \mu\text{m}$. This value will thus correspond to our lower-limit for the spatial resolution. Therefore, in order to excite one nanoantenna at a time, only devices with $d = 1000\text{ nm}$ have been analyzed.

By increasing the inter-antenna distance d , the nanoantennas loose most of their capability to increase the absorption in the NW. However, still for $d = 1000\text{ nm}$ there is an absorption mode at $\lambda = 750\text{ nm}$ that enhances the NW absorption efficiency. Therefore we set this wavelength to investigate the photo-carrier generation in the system for both s and p-polarizations.

We report the photo-current map related to transverse polarized incident light at $\lambda = 750\text{ nm}$ in Fig. 5a. The GaAs NW and antenna positions have been overlayed for clarity. The device is excited by a laser power of $18\ \mu\text{W}$ and 50 mV are also applied at the electrodes in order to extract the photo-carriers. The blue region in the contour plot corresponds to the area where the laser is not probing the NW, thus is related to the dark current. When the laser spot is on the NW the current increases due to the generation of photo-carriers. It is worth to notice that there is no Schottky barrier in proximity to the contacts, which indicates that any effects related to the contacts can be excluded.

It is also interesting to notice that the photo-current is not homogeneous along the NW. In particular, we observe an enhancement of photo-current right in the vicinity of the nanoantennas position. This trend is more clear by plotting the photo-current profile along the NW (Fig. 5b). We also include the photo-current profile given by longitudinal polarized light. At first sight, one can already observe that the two photo-current profiles are different at the position of the nano-antenna. In order to explain this phenomenon, let us distinguish between the laser spot being on the nanoantenna (region 1) and when located between two nanoantennas (region 2). In the profile for the s-polarised light, the photo-current is always enhanced in regions of type 1, while is reduced in regions of type 2. We notice that, the

nanoantennas adjacent to the electrical contacts give a smaller contribution to the creation of photo-carriers. The close presence of the contacts change the light coupling which becomes less efficient.

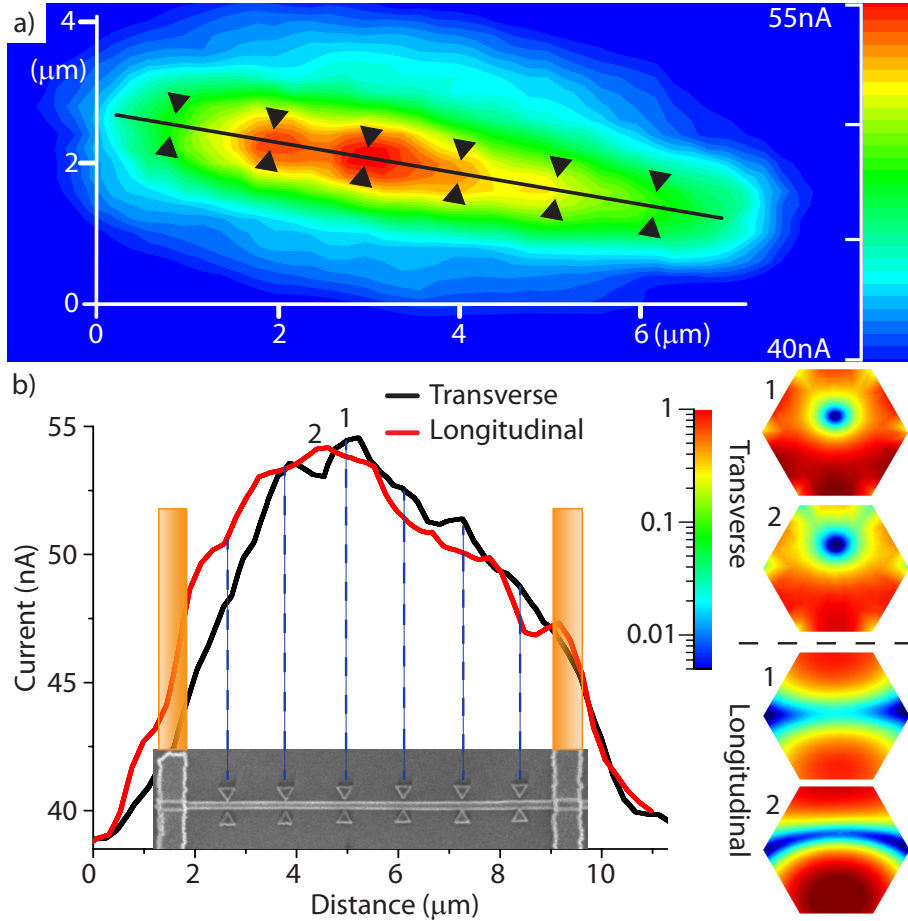


FIG. 5. a) 2D photo-current map of a system $d = 1000 \text{ nm}$ with 6 nanoantennas represented in back. A super-continuum laser and a piezo-stage are used to scan the device with incident transverse polarized light with $\lambda = 750 \text{ nm}$. The different colors correspond to different photo-current levels: blue the lowest and white the highest. b) Current profile along the NW axis for transverse polarized (black) and longitudinally polarized (red) light with $\lambda = 750 \text{ nm}$. The SEM shows the position of the contacts and the nanoantennas. On the left, the simulated field energy distribution along the NW cross section for both polarizations in 2 different positions: 1) on the nanoantenna position and 2) at half way between 2 nanoantennas. The color scale is in logarithmic values.

SI 5: Raman scan

In order to further demonstrate the local nanoantenna effect we performed Raman scans along the nanowire/nanoantennas system with nanoantenna distance $d = 1000 \text{ nm}$ for longitudinal and transverse polarization (fig. 6a and 6b). An $Ar^+ - Kr^+$ laser is used to excite the nanowire with 647 nm wavelength. The excitation beam has a power of $400 \mu W$ and it is focused with a spot size of around $1 \mu m$ by a 100X objective (NA 0.75), leading to $5 \cdot 10^4 \text{ W/cm}^2$. Although this wavelength does not correspond to the system maximum absorption (fig. 2 of the main test) and therefore the nanoantennas effect is not optimized, the Raman scanning shows a different behavior for longitudinal and transverse polarized light. For longitudinal polarization the TO Raman peak is homogeneous along the full nanowire, on the other hand, transverse polarization shows peaks of intensity between the nanoantennas confirming the dipole nature of the bow-tie antennas.

We want to highlight that the bow-tie antennas array is not efficiently coupling and concentrating the light into the nanowire at 647 nm wavelength, but by looking at the Raman scans we investigate the periodicity of the system and observe different TO intensity in function of the nanoantennas position (fig. 6b). The nanoantennas ability to modulate the nanowire absorption makes Raman measurements crucial for the understanding of new physical properties. The reduction or enhancement of Raman peak transitions will bring more light into the complex coupling between semiconductor nanowires and optical antennas.

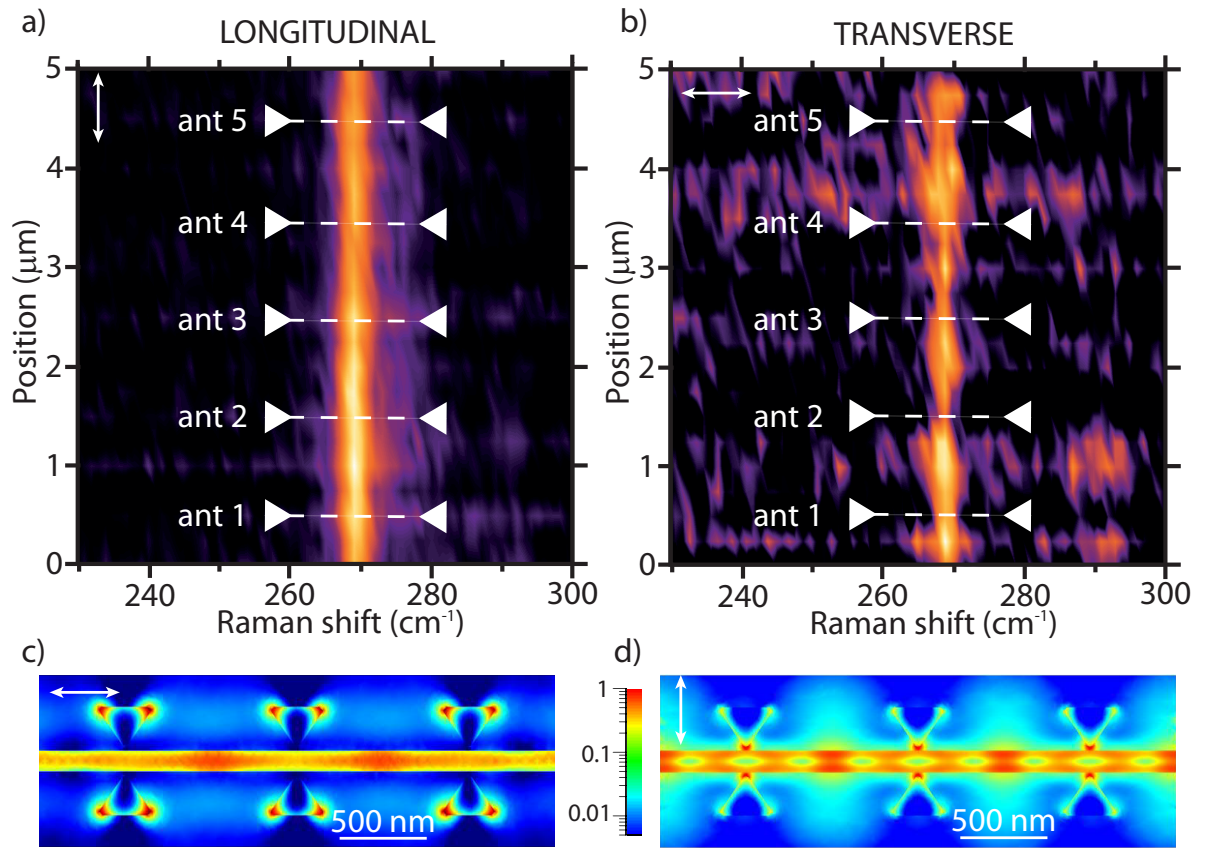


FIG. 6. a) and b) show the Raman shift line scan along the NW for longitudinal and transverse polarization at 647 nm wavelength. The nanoantennas are represented on top of the images and their distance is 1000 nm. c) and d) field energy map for the analyzed device with longitudinal and transverse polarization.